Journal of Electroceramics, Volume 20, Number 1, February 2008, pp53-58

Direct and converse magnetoelectric effect at resonant frequency in laminar piezoelectric-magnetostrictive composite

C. Popov[2], H. Chang[1], P.M. Record[2], E. Abraham[2], R.W. Whatmore[1,3] and Z. Huang[1,*]

[1]*Department of Materials, School of Applied Science, Cranfield University, Beds, MK43 0AL, UK*

[2]*School of Engineering and Physical Sciences, Heriot-Watt University, Edinburgh EH14 4AS, UK*

[3]*Current Address: Tyndall National Institute, Cork, Ireland.*

[*]*Corresponding author e-mail: Z.Huang@cranfield.ac.uk*

Abstract

Laminar piezoelectric-magnetostrictive composites using piezoelectric lead zirconate titanate ceramics and the giant magnetostrictive rare-earth-iron alloy Terfenol-D were prepared by epoxy bonding. The direct and converse magnetoelectric (ME) effects at and off the mechanical resonant frequency were characterized and compared to the theoretical modelling. The mechanical resonant frequency of the composites depended on the sample orientation and the magnetic DC bias field. In the longitudinal configuration, the resonant frequency shifted down monotonically with the increasing bias field. When the sample was in the transverse configuration, the resonant frequency decreased with the increasing field at first. However, at higher bias, it shifted up with the increasing bias. A phenomenological model based on the ΔE effect of magnetostrictive materials is proposed to explain the observed phenomena.

Keywords: magnetoelectric effect, piezoelectric, magnetostrictive, PZT, ΔE effect, orientation dependence.

1. Introduction

The fact that the magnetisation of a magnetic material can be controlled by an external magnetic field is widely used in today's information technology. The manipulation of magnetisation by means other than magnetic field, for example electric field, could find applications in magnetic storage, spintronics [1], and other magnetic sensing and actuating micro-electric-mechanical systems (MEMS) devices [2]. Electrically-controlled magnetic switches have been reported recently in the hole-induced ferromagnetic semiconductor (In,Mn)As [3] and the magnetic ferroelectric compound $HoMnO_3$ [4] via magnetoelectric interaction. However, both of these were observed at very low temperatures (less than 25K). Recently, electrically tunable ferromagnetic resonance [5,6] via magnetoelectric (ME) interaction and the converse ME effect at low frequency [7] have been reported.

The ME effect is characterized by the appearance of an electric polarization on applying a magnetic filed ($\alpha=\delta\mathbf{P}/\delta\mathbf{H}$, called the ME_H effect, or direct ME effect) or by the appearance of a magnetization on applying an electric field ($\alpha=\delta\mathbf{M}/\delta\mathbf{E}$, called ME_E effect, or converse ME effect). It was foreseen by Landau and Lifshitz from thermodynamics and symmetry consideration [8] and was first measured in a Cr_2O_3 crystal [9,10]. The ME effect in single phase materials is usually very small and often can only be realised at very low temperatures [11,12].

The ME effect can also be realised through product property [13]. Van Suchtelen proposed the product property concept whereby entirely new properties could be achieved by coupling a pair of tensor properties in two materials that were intimately mixed [13]. Since then two main processing routes have been investigated to achieve ME effect this way, namely, (a) particulate magnetostrictive (MS) and piezoelectric (PE) and (b) laminated MS/PE composites. Investigations on eutectic co-existing phases of spinel cobalt ferrite-cobalt titanate and perovskite barium titanate

achieved magnetoelectric voltage coefficient $\alpha_E = \alpha/\varepsilon_0\varepsilon_r \sim 50$ mV/cm Oe despite theoretical estimation to be 40-60 times larger [14], where ε_r is the relative permittivity and ε_0 the dielectric constant of vacuum. Similar ME coefficient were obtained with particulate composites of the giant MS rare-earth-iron alloy $Tb_{1-x}Dy_xFe_2$ (TFD) and lead zirconate titanate (PZT) and PVDF polymer [15]. A recent investigation of $CoFe_2O_4$-$BiFeO_3$ nanocomposites obtained α_E as high as 280 mV/cm Oe [16]. On the other hand, laminated MS/PE structures have been found to show much higher ME_H coefficients. α_E values of 1500 mV/cm Oe for ferrite-PZT [17] and 4680 mV/cm Oe for TFD/PZT laminar structures [18] have been reported. Significant enhancement of ME_H response can be obtained when the modulation frequency of the applied fields coincides with magnetic, electrical or mechanical eigenmodes of the system under study [19-21]. Here, we report the investigation of the direct and converse ME effects in composites at and off their mechanical resonant frequencies and the comparison between these measurement results and the theoretical modelling.

2. Experimental

The giant magnetostrictive rare-earth-iron alloy TFD (Gansu Tianxing Rare Earth Functional Materials Co, China) and the piezoelectric PZT ceramics (Ferroperm Piezoceramics, PZ29) were used to make laminar sandwich structures TFD/PZT/TFD and PZT/TFD/PZT by epoxy bonding (EPOTEK 301-2) at 85ºC . Meso-scale samples, with total thickness of 1.262 mm were fabricated by polishing down the TFD and then cutting the laminated composites. The PZT thickness was 0.127 mm, and the epoxy layer thickness was about 0.01 mm. The laminar was suspended between two thin Cu wires attached to the face centres. These two wires also served as two electrodes. This mounting allowed minimum physical clamping on the sample.

The direct ME effect was measured using an AC magnetic field generated from a Helmholtz coil as input and measure the induced electric voltage across the PZT as the output. The characterisation of the converse ME effect, namely, the electric voltage applied to the PZT as the input and the induced magnetisation of the TFD as the output, was carried out using a set-up similar for the direct ME measurement, without the Helmholtz coil. A sinusoidal voltage was applied to the PZT, and the induced AC magnetic field was measured by a pickup coil placed immediately outside the sample. Two pickup coils placed at perpendicular directions at the same time were used for the three dimensional characterisation of the induced magnetisation field. The DC bias magnetic fields were provided by a pair of electromagnet. For all measurements presented here, the AC and DC magnetic fields were parallel. At high frequency the inductance of the Helmholtz coil generates a prohibitively large voltage so for frequencies above 10kHz the inductance was tuned out by a series variable capacitance. The total capacitance required to put the coils in resonance was calculated from the inductance and resistance measured with RCL Bridge (Fluke, PM6306). For frequencies below 10kHz the Helmholtz coil pair was driven directly. More experimental details can be found elsewhere [22]. The longitudinal and transverse measurement configurations have been investigated, as schematically shown in Fig. 1.

3. Results and Discussion

Fig. 2a shows typical ME response as a function of frequency at transverse configuration. At low frequencies (<40KHz) the ME voltage coefficient $\alpha_v = E/H$ was almost a constant. The α_v was found to depend on the DC bias field, and had the highest value for the bias field around 400 Oe. This is understandable since the ME coefficient is proportional to the MS coefficient q_{31}, and q_{31} reaches its maximum at H_{dc} around 350 Oe [23]. The α_v had a sharp increase around the resonant frequency. The nature of this resonance was dominated by mechanical effect, as can be confirmed

from the following calculation: Let f_r be the fundamental mechanical resonant frequency of the bonded structure, and assuming the bonding is perfect and had negligible thickness, then [24]

$$f_r = \frac{1}{2l}\sqrt{\frac{v_{PZT}Y_{pzt} + v_{tfd}Y_{tfd}}{\rho_{PZT}v_{PZT} + \rho_{tfd}v_{tfd}}} \qquad (1)$$

Here l=14.5mm was the sample length. Using material parameters Young's modulus Y_{tfd}=4x10^{10} Nm^{-2}, Y_{pzt}=5.9x10^{10} Nm^{-2}, volume fraction v_{tfd}=0.9, vt_{pzt}=0.1, density ρ_{tfd}=9.2Kg m^{-3} and ρ_{pzt}=7.46Kg m^{-3} it can be obtained f_r =74.3KHz, which agrees well with the observed values. The peak height of the α_v at resonance was found to depend on the DC and AC magnetic fields, the sample orientation, as well as the particular sample (Fig.2b, another sample), a value up to α_v =90 V cm^{-1}Oe^{-1} has been observed at the resonance. The linearity between the voltage output across the PZT and the magnetic AC field applied to the TFD has been confirmed for both the low frequency and resonant responses. Unlike the low frequency response, the α_v at resonance was found to increase with the bias field up to H_{dc}=1000 Oe, which was the maximum bias field used in this experiment. The α_v was measured as 11.3 V cm^{-1}Oe^{-1} at 70KHz at the DC bias 300 Oe. From Fig. 1a curve's behaviours this suggested α_v about 11.3/3 = 3.8 V cm^{-1}Oe^{-1} at low frequency (<40KHz). Using equation (13) in Ref 25 and material parameters listed in the Table I, the calculated ME voltage coefficient is α_v=8.2 V cm^{-1}Oe^{-1} which agrees well with the measured value.

Similar to the direct ME effect, the converse ME response was nearly a constant at low frequency (<40KHz), and the ME Oersterd coefficient [26] α_H = M/E was measured as 9 Oe cm/KV (assuming μ_r=1) at 70KHz for a bias field of 300 Oe, here M is the induced magnetisation in the TFD and E the electric field across the PZT. The α_H also peaked at the resonance frequency (79KHz) with a value of 50 Oe cm/KV (Fig. 3). The theoretically calculated value is 19 Oe cm/KV at low frequency (well below resonance) if the bonding is assumed to be perfect [26]. Both the

calculated and the measured values were more than 3 orders of magnitude larger than the value for Cr_2O_3 for which the α_H is no more than 41 $x10^{-4}$ Oe cm/KV.

Another interesting feature of the ME effect is the shift of the resonant frequency with the applied magnetic bias field. Fig. 4 and Fig. 2 show the resonant frequency dependence on the bias field for (a) the longitudinal and (b) transverse configurations for different AC fields respectively. In the longitudinal configuration, the sample's length, which was also the easy axis of the TFD was perpendicular to the DC and AC magnetic fields, the resonant frequency shifted lower monotonically with the increasing bias field (Fig. 5a). When the sample was in the transverse configuration, the sample's length and therefore the easy axis was parallel to the DC and AC magnetic fields. At small DC bias field, the resonant frequency decreased with the increasing field. However, at higher bias, it shifted up with the increasing bias (Fig. 5b). For the converse ME response (Fig. 3), the resonant frequency shift as a function of the magnetic bias field was similar to those observed in the direct ME effect. This dependence of resonant frequency on the bias magnetic field is consistent with the ΔE effect, which is the dependence of the Young's modulus of the MS materials on the magnetic field. For MS materials, the strain produced by the MS effect adds to the stress-induced strain, so the material becomes softer when the magnetic moments are free to rotate. It becomes increasingly stiff when approaching saturation and magnetic moment mobility decreases. Squire [27] developed a phenomenological model for the ΔE effect and we use this model to explain the above observed results.

In eqn (1), Y_{pzt} and ρ_{pzt} does not change with magnetic field since the PZT is not a magnetic material, and v_{tfd}, v_{pzt} and ρ_{tfd} do not change much since the volume change with magnetic field is close to zero. Therefore, we can discuss the dependence of Y_{tfd} on the magnetic field directly. According to Squire [27], $\frac{Y}{Y_s} = \frac{1}{1+(9\lambda_s^2 Y_s / 8K)F(h,\theta,\gamma)}$, here λ_s, Y_s and K are respectively the MS coefficient at saturation, Young's modulus at saturation and anisotropy energy density of the TFD.

$F(h, \theta,\gamma)$ is a function of the reduced magnetic field $h=H\mu_0 M_s/2K$, reduced strain energy $\gamma=3\lambda_s\sigma/4K$, and wall angle θ between the easy axis and the external field direction. At the longitudinal configuration, θ=90°, the magnetisation is by means of moment rotation only and its Young's modulus decreases monotonically until saturation at h=1. At the transverse configuration, θ=0°, the magnetisation is by means of domain wall movement only and its Young's modulus increases monotonically with the increasing bias field. Squire's model has singularity at θ=0° so a small θ (e.g. 15°) is used for the numerical calculation. Fig. 5c depicts the calculated Y_{tfd}/Y_s as functions of the reduced bias field for θ=90° (solid line) and θ=15° (dotted line). For our sample, the TFD was most likely to be composed of both the θ =90° and θ=0° domains at both the transverse and longitudinal configurations, due to the existence of an internal stress developed during the cooling of the sandwiched structure to room temperature from the curing temperature (85°C). TFD has a much larger thermal expansion coefficient than the PZT, so at room temperature the TFD was under tensile and the PZT under compressive stresses. Assuming α is the thermal expansion coefficient, then the stress:

$$\sigma = \frac{t_{pzt} Y_{pzt} * Y_{tfd}}{(t_{tfd} Y_{tfd} + t_{pzt} Y_{pzt})} * (\alpha_{pzt} - \alpha_{tfd}) * (T_2 - T_1)$$

using α_{tfd}=11x10^{-6} K^{-1}, α_{pzt}=2x10^{-6} K^{-1} , Y_{tfd}=4x10^{10} Nm^{-2} , Y_{pzt}=5.9x10^{10} Nm^{-2}, t_{tfd}=1.12 mm, t_{pzt}=0.127 mm, T_2=85 °C, T_1=20 °C, we obtain σ= 3.3 x 10^6 Nm^{-2}. The stress induced magnetisation due to the Villari effect in the TFD can then be obtained from $B_j=q_{ij}T_j$. From the manufacturer's data curve, this corresponds to 13.5KA/m=170 Oe. The measured value (85 Oe) agrees well with the above calculation. If we assume there were 80% and 20% of the θ =90° and θ =0° domains in the longitudinal configuration and 20% and 80% in the transverse configuration, respectively, the calculated Y_{tfd}/Y_s as functions of the reduced bias field are depicted in the Fig. 5c as the dashed line and broken line respectively. These two profiles agree qualitatively well with our experimental observations.

4. Summary

Laminar piezoelectric-magnetostrictive composites using piezoelectric lead zirconate titanate and the giant magnetostrictive rare-earth-iron alloy Terfenol-D were prepared using epoxy bonding. The

direct and converse magnetoelectric (ME) effects at and off the mechanical resonant frequency were characterized and compared to theoretical modelling. The mechanical resonant frequency of the composites was observed to depend on the sample orientations as well as the magnetic DC bias field. In the longitudinal configuration, the magnetic easy axis of the TFD was perpendicular to the DC and AC magnetic fields, the resonant frequency shifted down monotonically with the increasing bias field. When the sample was in the transverse configuration, the easy axis of the TFD was parllel to the DC and AC magnetic fields, the resonant frequency decreased with the increasing field initially. However, at higher bias field, it shifted up with the increasing bias. A phenomenological model based on ΔE effect of magnetostrictive materials is proposed to explain the observed phenomena.

Acknowledgement

This work was financially supported by the UK EPSRC Grants GR/R92448, EP/D506638/1 and EP/C519426/1.

References

[1] G. A. Prinz, *Science*, **282**, 1660-1663 (1998).

[2] M. Fiebig, *J. Phys.D: Appl. Phys.* **38**, R123-152 (2005).

[3] H. Ohno, D. Chiba, F. Matsukura, T. Omiya, E. Abe, T. Diett, Y. Ohno, and K. Ohtani, , *Nature* **408**, 944-946 (2000).

[4] T. Lottermoser, T. Lonkal, U. Amann, D. Hohlwein, J. Ihringer, and M. Fiebig, *Nature* **430**, 541-544 (2004).

[5] A.A. Semenov, S.F. Karmanenko, V.E. Demidov, B.A. Kalinikos, G. Srinivasan, A.N. Slavin, and J.V. Mantese, *Appl. Phys. Lett.*, **88**, 033503 (2006).

[6] Y. K. Fetisov and G. Srinivasan, *Appl. Phys. Lett*., **88**, 143503 (2006).

[7] Y. Jia, S.W. Or, H.L.W. Chan, X. Zhao and H. Luo, *Appl. Phys. Lett*., **88**, 242902 (2006).

[8] L.D. Landau and E. M. Lifshitz, "*Electrodynamics of Continous Media*," Pergamon Press, Oxford (1960) (Translation of Russian Edition, 1958).

[9] D.N. Astrov, *Zh. Exp. Teor. Fiz.*, **37,** 881 (1959) [*Soviet Phys.-JETP*, **10**, 628 (1960)].

[10] V.J. Folen, G.T. Rado and E.W. Stalder, *Phys. Rew. Lett*., **6**, 607 (1961).

[11] G.T. Rado, J.M. Ferrari, and W.G. Maisch, *Phys. Rew*. **B29**, 4041 (1984).

[12] K. Agyei and J. L. Birman, *J. Phys.: Condens. Matter*., **2**, 3007 (1990).

[13] J. van Suchtelen, *Philips Res. Rep.*, **27**, 28 (1972).

[14] J. van den Boomgaard, D.R. Terrell, R.A.J. Born and H.F.J.I. Giller, *J. Mater. Sci*., **9**, 1705 (1974); A.M.J.G. van Run, D.R. Terrell, and J.H. Scholing, *J. Mater. Sci*., **9**, 1710 (1974).

[15] C.W. Nan, N. Cai, L. Liu, J. Zhai, Y. Ye and Y. Liu, *J. Appl. Phys*., **94**(9), 5930 (2003).

[16] X. Liu, S. Fu and C. Huang, *Mater. Sci. & Engin*., **B121**, 255 (2005).

[17] G. Srinivasan, E.T. Rasmussen, J. Gallegos, R. Srinivasan, Yu.I. Bokhan, and V.M. Laletin, *Phys. Rev.* B**64**, 214408 (2001)

[18] J. Ryu, A.V. Carazo, K. Uchino, and H.E. Kim, *Jpn. J. Appl. Phys., Part 1*, **40**, 4948 (2001).

[19] U. Laletsin, N. Padubnaya, G. Srinivasan and C.P. Devreugd, *Appl. Phys.* **A78**, 33 (2004).

[20] S. Dong, J. Li, and D. Viehland, *App. Phys. Lett.* **83**, 11 (2003).

[21] S. Dong, J. Li, and D. Viehland, *App. Phys. Lett.* **86**, 182506 (2005).

[22] P.M. Record, C. Popov, E. Abraham, J. Fletcher, H. Chang, Z. Huang and R.W. Whatmore, *submitted to Sensors and Actuators A-Physical.*

[23] The magnetostriction ($\lambda_{//}$) data as supplied by the manufacturer as a function of magnetic field was approximated by a polynomial fitting, then its derivation which should equal the q_{33} was obtained. q_{31} was obtained by assuming $q_{31}= -q_{33}/2$.

[24] S. Schmidt and C.A. Grimes, *IEEE Trans. Mag.* **37,** 2731-2733 (2001).

[25] M.I. Bichurin and V.M. Petrov, *Phys. Rew. B*, **68**, 054402 (2003).

[26] Z. Huang, *J. Appl. Phys*, **100**, 114104 (2006).

[27] P.T. Squire, *J. Magn. Magn. Mat.*, **87**, 299-310 (1990).

Figure captions

Fig. 1 Schematic of the configurations for (a) transverse; (b) longitudinal; and (c) converse ME effect measurements.

Fig. 2 Magnetoelectric voltage coefficients α_v as functions of frequency: (a) in the full frequency range 100-100KHz for one sample and (b) around resonant frequency for different DC bias fields for a transversely oriented TFD-PZT-TFD composite.

Fig. 3 Magnetoelectric Ostered coefficients α_H as functions of frequency for different DC bias fields for a transversely oriented TFD-PZT-TFD composite.

Fig. 4 Magnetoelectric voltage coefficients α_v as functions of frequency for different DC bias fields for a longitudinal oriented TFD-PZT-TFD composite.

Fig. 5 Magnetic bias field dependence of the resonant frequency for the (a) longitudinal and (b) transverse configuration with different ac fields. (c) phenomenological modelling of the Young's modulus for the longitudinal (θ=90° domain) and transverse (θ=0° domain) and mix oriented samples.

Table I: Material parameters used for the numerical calculation

for lead zirconate titanate (PZT) and Terfenol-D (TFD).

	TFD	PZT
Length (10^{-3} m)	14.5	14.5
Thickness (10^{-3} m)	0.56	0.127
Density (Kg/m^3)	9200	7460
$s_{11(}10^{-12}m^2/N$)	25	17
$s_{12(}10^{-12}m^2/N$)	-1.8	-5.8
$s_{13(}10^{-12}m^2/N$)	-16.7	-8.8
$s_{33(}10^{-12}m^2/N$)	40	22.9
$d_{31}(10^{-12}m/V)$		-243
$d_{33}(10^{-12}m/V)$		574
$q_{31}(10^{-9}m/A)$	-13	
$q_{33}(10^{-9}m/A)$	26	
ε_{33}		2870

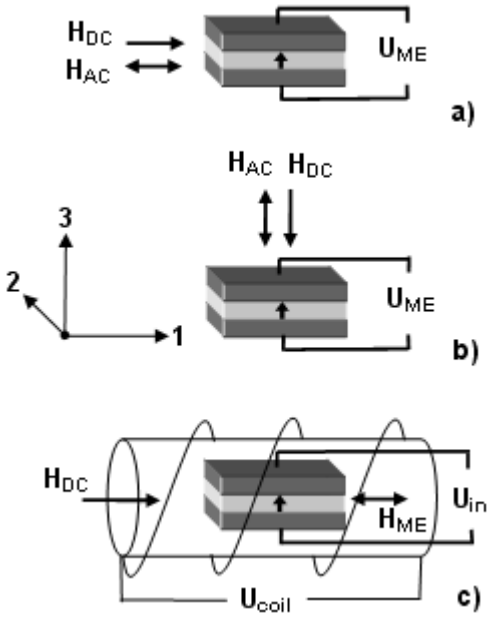
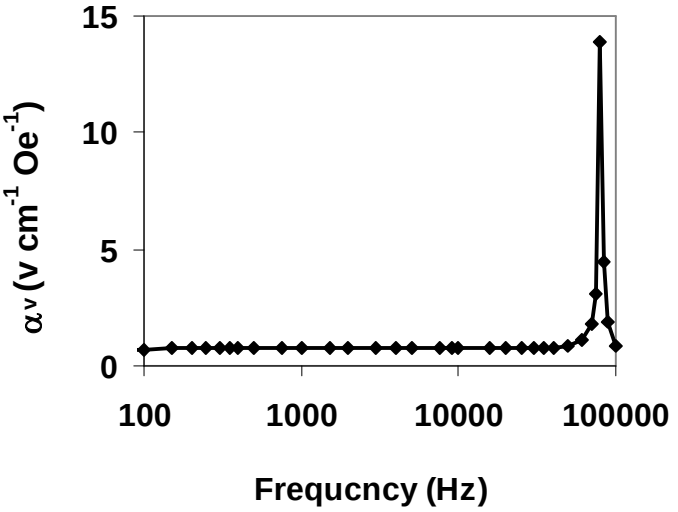


Fig. 1


15
10
5
0
100
1000
10000
100000
αv (v cm-1 Oe-1)
Frequcncy (Hz)

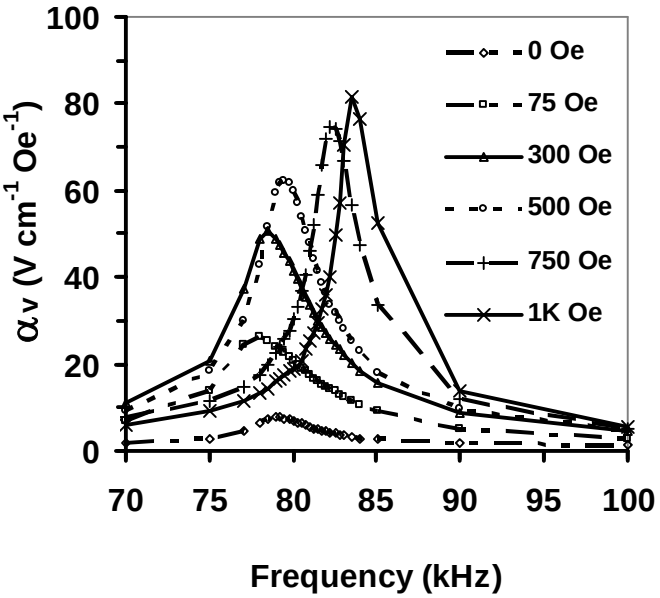

100
80
60
40
20
0
70
75
80
85
90
95
100
αv (V cm-1 Oe-1)
Frequency (kHz)
0 Oe
75 Oe
300 Oe
500 Oe
750 Oe
1K Oe

Fig. 2

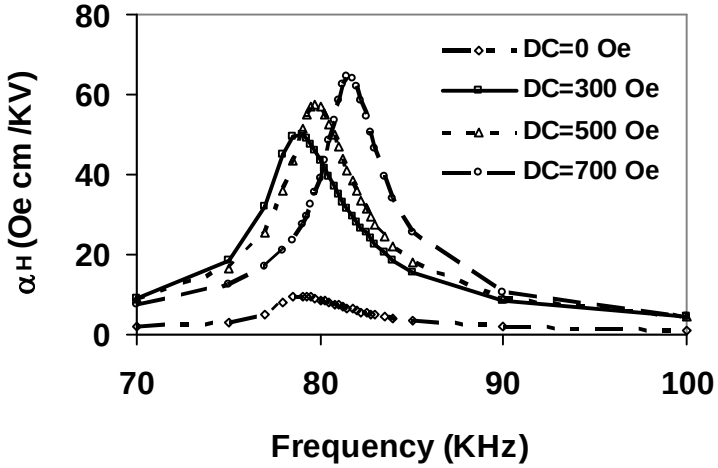

80
60
40
20
0
αH (Oe cm /KV)
DC=0 Oe
DC=300 Oe
DC=500 Oe
DC=700 Oe
70
80
90
100
Frequency (KHz)

Fig. 3

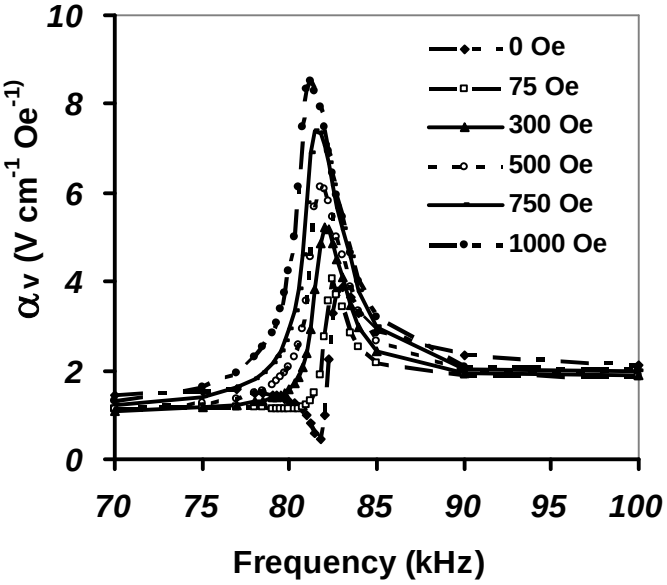

10
8
6
4
2
0
αv (V cm-1 Oe-1)
0 Oe
75 Oe
300 Oe
500 Oe
750 Oe
1000 Oe
70
75
80
85
90
95
100
Frequency (kHz)

Fig. 4

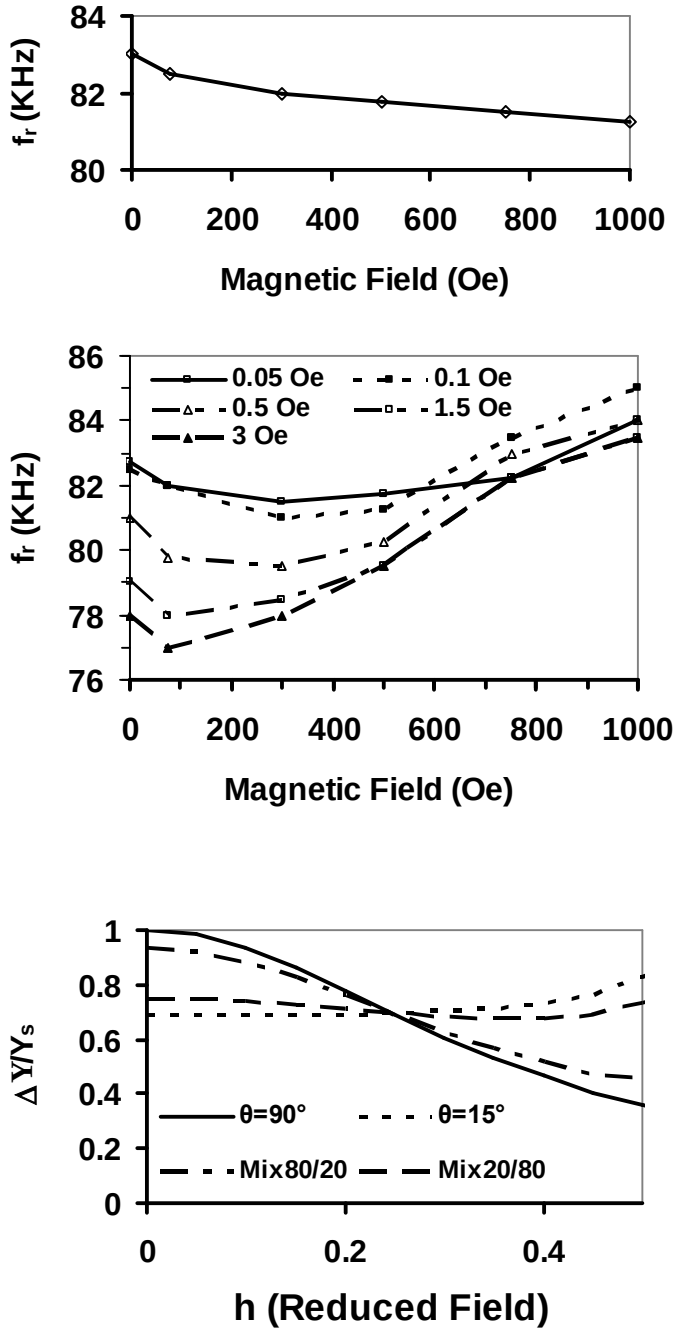

84
82
80
f_r (KHz)
0
200
400
600
800
1000
Magnetic Field (Oe)
86
84
82
80
78
76
f_r (KHz)
0.05 Oe
0.1 Oe
0.5 Oe
1.5 Oe
3 Oe
0
200
400
600
800
1000
Magnetic Field (Oe)
1
0.8
0.6
0.4
0.2
0
$\Delta Y/Y_s$
θ=90°
θ=15°
Mix80/20
Mix20/80
0
0.2
0.4
h (Reduced Field)

Fig. 5



https://dspace.org/

Direct and converse magnetoelectric effect at resonant frequency in laminar piezoelectric-magnetostrictive composite.

Popov, C.; Chang, Harrison Hoon Seok; Record, P. M.; Abraham, E.; Whatmore, Roger W. ...

2008-02-01T00:00:00Z
Springer Science Business Media
http://dx.doi.org/10.1007/s10832-007-9184-5
C. Popov, H. Chang, P. M. Record, E. Abraham, R. W. Whatmore1, and Z. Huang, Direct and converse magnetoelectric effect at resonant frequency in laminar piezoelectric-magnetostrictive composite. Journal of Electroceramics, Volume 20, Number 1, February, 2008, pp53-58

Downloaded from a DSpace repository. https://dspace.org/